

**Measuring a completely unknown phase with sub-shot-noise precision in the presence of loss**

N. Gkortsilas, J. J. Cooper, and J. A. Dunningham

*School of Physics and Astronomy, University of Leeds, Leeds LS2 9JT, United Kingdom*

(Received 23 February 2012; published 22 June 2012)

We present a practical scheme for measuring completely unknown phases with a precision beyond the shot-noise limit even in the presence of loss. Our scheme consists of sending a sequence of unentangled particles and NOON states through an interferometer and analyzing the measurement outcomes using a Bayesian analysis. We compare our results with two recent schemes [L. Pezzé and A. Smerzi, *Europhys. Lett.* **78**, 30004 (2007); B. L. Higgins *et al.*, *Nature (London)* **450**, 393 (2007)] that are closely related but operate in the lossless regime. We show that our technique outperforms the previous schemes when even a modest amount of loss is present and so may prove to be a valuable technique for making precision measurements beyond the classical limit in a range of practical scenarios.

DOI: [10.1103/PhysRevA.85.063827](https://doi.org/10.1103/PhysRevA.85.063827)

PACS number(s): 42.50.St, 03.67.Bg, 06.20.-f, 03.65.Yz

**I. INTRODUCTION**

The ability to make evermore precise measurements of physical quantities lies at the heart of progress of science. Since the precision that can be achieved in a measurement is related to the resources we have at our disposal, there are two key ways we can improve measurements: either we use more resources or we use our resources more efficiently. The first approach can be understood by the fact that, if we repeat a measurement many times, we improve the statistics and hence glean more information about the unknown quantity. A stream of  $N$  independent particles, for example, would enable us to make  $N$  separate interactions with the system and  $N$  separate measurements. This approach is commonly used in interferometry, for example, and gives a precision that scales as  $1/\sqrt{N}$ . This is called the shot-noise limit and arises from the inevitable “jitter” in the measurement outcomes due to the discreteness of the particles.

The second approach involves using the resources more efficiently, which can be achieved by entangling them. This is the field of quantum metrology and is one of the most exciting emerging applications of quantum entanglement [1–4]. For linear systems with no loss, it can be shown that the measurement precision using entanglement can scale as  $1/N$ , and for systems with interactions between the particles, the scaling can be even more favorable [5]. This suggests that there is a lot to gain from entanglement. However, the problem is that any realistic system contains loss, and it is well known that loss undermines the advantage gained by entanglement [6]. Indeed it has been shown recently that in the limit  $N \rightarrow \infty$ , if there is any loss in the system, the best precision that can be obtained is reduced to a small numerical factor improvement over the unentangled case, i.e.,  $1/\sqrt{N}$  [7–9]. Nonetheless, the value of  $N$  at which this crossover to unentangled behavior occurs can be quite large, and so it is still very fruitful to study quantum metrology for entangled states with a modest number of particles. This means that quantum metrology schemes are likely to come into their own when there are reasons we might want to limit the resources we use, for example, if we are imaging a delicate sample that would be damaged by a high incident flux or trying to detect gravity waves where the signal is so small that photon pressure noise risks completely swamping it.

Most entanglement-based measurement schemes are somewhat limited in that they require the experimenter to initially know the phase that they wish to measure to a high degree of accuracy. This is not always practical or possible. However, recent work has shown how it is possible to achieve sub-shot-noise precision even when the initial phase is unknown. Pezzé and Smerzi (PS) developed a theoretical scheme that was able to achieve a measurement precision that scaled as  $1/N$  [10]. Higgins *et al.* (HBBWP) took this further and performed an experiment that used feedback to demonstrate sub-shot-noise scaling [11]. These are both beautiful demonstrations of the potential advantages of quantum metrology, but both operate in the lossless regime. In this paper we will extend these ideas to consider the effects of loss and demonstrate a simple scheme that outperforms them when there is more than a modest amount of loss present.

**II. THE SCHEME**

The basic measurement scheme is shown in Fig. 1. It consists of a device that creates a (single particle or multiparticle) superposition on the two paths. One path is then subjected to the phase shift  $\phi$  that we wish to measure before a second device undoes the effect of the first one. Finally, particles are detected at the two output ports, D1 and D2. This is really just a generalized Mach-Zehnder interferometer that admits multiparticle entangled states on the two paths.

In the lossless case without interactions between the particles, it is known that the best possible measurement precision is given when the first device creates the NOON state  $|\psi\rangle = (|N_e, 0\rangle + |0, N_e\rangle)/\sqrt{2}$  on the two paths. There are schemes for performing this transformation in optical [4,12] and atomic systems [13]. For our purposes, we want this process to be unitary, which can be achieved by using a nonlinearity as described in [13,14]. An alternative used in the HBBWP scheme was to create a single-particle superposition using an ordinary beam splitter and then to pass it through the phase shift multiple times [11]. This is a clever idea that simplifies experimental implementations but suffers from a bandwidth problem in the sense that the time to make a measurement scales with  $N_e$ . The same is not true for NOON states where the measurement time is independent of  $N_e$ .

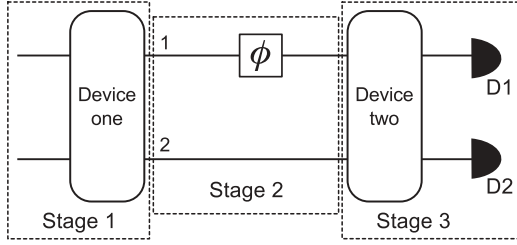


FIG. 1. A schematic of the phase measurement scheme. In stage 1 the input state is transformed unitarily by device 1 to some superposition state on the two paths. In stage 2, one of the two modes acquires the phase  $\phi$  that we wish to measure. Finally, in stage 3, device 2 undoes the transformation of device 1, and particles are detected at D1 and D2 with probabilities that depend on  $\phi$ . In a standard Mach-Zehnder interferometer devices 1 and 2 would simply be 50:50 beam splitters.

If the NOON state is propagated through the scheme shown in Fig. 1, the output state (ignoring a global phase) is  $|\psi\rangle = \cos(N_e\phi/2)|N_e, 0\rangle + \sin(N_e\phi/2)|0, N_e\rangle$ . From this we see that all particles are detected at D1 with probability  $P_1 = \cos^2(N_e\phi/2)$  or all at output D2 with probability  $P_2 = \sin^2(N_e\phi/2)$ , which allows us to estimate the phase  $\phi$ .

The probability of detecting the  $N_e$  particles at either of the two output ports has a period of  $2\pi/N_e$ , and so we can measure the phase  $\phi$  to within  $2\pi/N_e$ . However, the periodicity means that we are not able to distinguish phases that differ by multiples of  $2\pi/N_e$ . This is a problem if the phase is initially completely unknown: we need to know in which  $2\pi/N_e$  period  $\phi$  lies.

One possible way to do this is to make a simple initial measurement of  $\phi$  using unentangled particles. This is achieved by inputting  $|N_u, 0\rangle$  into a standard Mach-Zehnder interferometer and recording the number of particles detected at D1 and D2. Each particle has a probability  $P_1 = \cos^2(\phi/2)$  of being detected at D1 and  $P_2 = \sin^2(\phi/2)$  of being detected at D2. This means that (unlike for the NOON state) the probability distribution has a single peak on the  $2\pi$  range, and so  $\phi$  can be uniquely identified. In this case the measurement precision is limited by shot noise, i.e.,  $\Delta\phi \geq 1/\sqrt{N_u}$ . Therefore, in order to narrow down our estimate of  $\phi$  to a  $2\pi/N_e$  period we require  $N_u \approx [N_e/(2\pi)]^2$  [15]. Since in any given experiment we have a fixed total number of particles, we ideally want  $N_u$  to be small so as to save as many particles as possible for the more precise NOON state measurement. In this paper we investigate this scheme to see how we can use a combination of  $N_u$  unentangled particles and  $\gamma$  copies of NOON states (each with  $N_e$  particles) to precisely measure an unknown phase in the presence of loss [16]. This means that the total resources are  $N_T = N_u + \gamma N_e$ .

### III. PHASE READOUT

The readout mechanism is a key part of any measurement scheme. Often in quantum metrology, the quantum Fisher information  $F_Q$  [17,18] and its associated Cramér-Rao bound  $\Delta\phi \geq 1/\sqrt{F_Q}$  [9,19–21] are used to quantify the precision that a given quantum state can achieve. However, this is a theoretical limit that is optimized over all possible readout

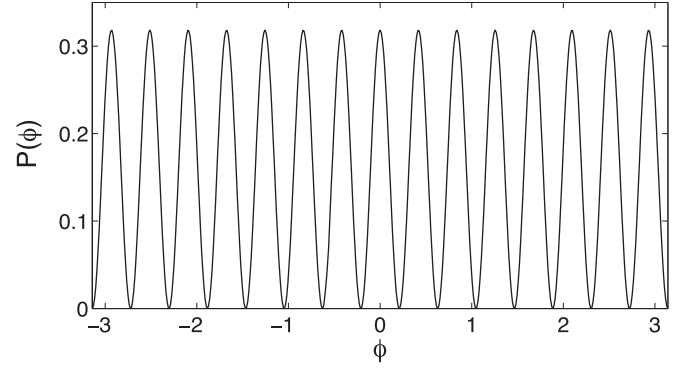


FIG. 2. The phase distribution resulting from using a single  $N_T = 15$  particle NOON state as the measurement resource. The periodicity of the distribution means that the phase can only be estimated modulo  $2\pi/N_T$ .

schemes, and often it is not at all clear how to implement the best possible case. Instead we take a more pragmatic approach and consider a particular readout scheme that was also used in the PS and HBBWP schemes. This should be useful in guiding possible experimental implementations. The readout scheme involves detecting particles at the outputs D1 and D2 and using Bayesian analysis to determine  $\phi$ .

It is helpful to start by reviewing this. In the PS scheme, a sequence of  $\nu$  NOON states with particle numbers  $N_e = 1, 2, 4, 8, \dots, 2^{\nu-1}$  were used to achieve a measurement precision  $\Delta\phi = 2.55/N_T$  when there is no loss and  $\phi = 0$ . As discussed above, detectors D1 and D2 in Fig. 1 will detect all the particles at either output 1 or 2 with respective probabilities  $P_1 = \cos^2(N_e\phi/2)$  and  $P_2 = \sin^2(N_e\phi/2)$ . Repeating for all  $\nu$  NOON states, the probability that  $x$  times we detect all the particles at output 1 and  $\nu - x$  times at output 2 can be written as  $P_\nu(x|N_T, \phi)$ , which is often called the forward probability. According to Bayes' theorem, the posterior probability  $P_\nu(\phi|N_T, x)$ , i.e., our knowledge of  $\phi$  given total resources  $N_T$  and  $x$  detections at output 1, is given by

$$P_\nu(\phi|N_T, x) = \frac{P_\nu(x|N_T, \phi)P(\phi)}{P(N_T, x)}, \quad (1)$$

where  $P(\phi)$  describes our prior knowledge of  $\phi$  and is completely flat for an unknown phase,  $P(\phi) = 1/(2\pi)$ .  $P(N_T, x)$  can be treated simply as a normalization constant. The value of  $\phi$  for which the distribution  $P_\nu(\phi|N_T, x)$  is maximum is taken to be our estimate of the phase  $\phi_{\text{est}}$ , and the uncertainty  $\Delta\phi$  is taken to be the one-standard-deviation confidence interval. This is the phase interval containing 68.27% of the phase distribution, i.e.,  $\int_{\phi_{\text{est}} - \Delta\phi}^{\phi_{\text{est}} + \Delta\phi} d\phi P_\nu(\phi|N_T, x) = 0.6827$ . For simplicity the PS scheme considered the case where  $x = \nu$ , which occurs with certainty for  $\phi = 0$ .

When all  $N_T$  particles are put into a single NOON state, all the particles will be detected at output 1 (since  $\phi = 0$ ), and our estimate of the phase is  $P(\phi) \cos^2(N_T\phi/2)$ , which is shown in Fig. 2 for  $N_T = 15$  and shows the  $2\pi/N_T$  periodicity issue discussed above. The PS scheme avoids this issue by using  $\nu$  NOON states with particle numbers that increase in a

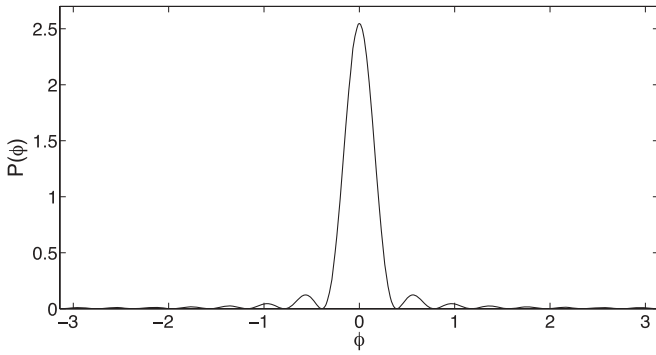


FIG. 3. The phase distribution resulting from the PS scheme [10] for  $\nu = 4$ ,  $N_T = 15$ . All the peaks except the one centered at the true phase value,  $\phi = 0$ , vanish.

geometric sequence as  $N_e = 1, 2, 4, 8, \dots, 2^{\nu-1}$ . This results in

$$P(\phi) \prod_{k=0}^{\nu-1} \cos^2\left(\frac{2^k \phi}{2}\right), \quad (2)$$

which is shown in Fig. 3 for  $\nu = 4$ . We see all the peaks, except the one centered at the true phase value, have been suppressed. This scheme should therefore allow us to unambiguously measure an unknown phase on the full  $2\pi$  period.

This is an interesting result, but it suffers from two problems. The first is that it does not account for loss. We know that loss will be present in any realistic system, and the fact that this scheme relies heavily on NOON states, which are known to be very fragile, suggests that it will be significantly degraded when loss is accounted for. This issue is addressed in Sec. V. The second problem is that the scheme only works when  $\phi = 0$ , so although it gives us a single peak in the  $2\pi$  range, it does not allow us to find a general unknown phase.

PS suggested how this scheme could be generalized to  $\phi \neq 0$  [10], and HBBWP found a clever solution by using an adaptive feedback mechanism [11]. A schematic of this idea is shown in Fig. 4. The unknown phase,  $\phi$ , on path 1 that we wish to measure can take any value, and a second phase,  $\theta$ , which is controlled by the experimenter, is placed on path 2. The PS scheme is then implemented with the difference that, after each detection, some information is gained about  $\phi$  and this is used to keep updating the value of  $\theta$  so that it always corresponds to our best estimate of  $\phi$ , i.e.,  $\phi_{\text{est}}$ . In this way, the phase difference between the two paths converges to a value close to zero, and this is the regime in which we

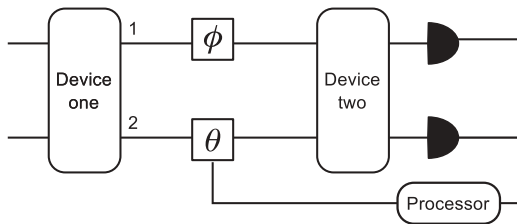


FIG. 4. A schematic of the measurement scheme with the feedback mechanism. Path 1 contains the phase  $\phi$  we wish to measure, and path 2 contains a known phase shift  $\theta$  that is adjusted after each detection so that it always corresponds to our best estimate of  $\phi$ , i.e.,  $\theta = \phi_{\text{est}}$ .

know that the PS scheme works. Of course there is some resource cost associated with this feedback mechanism. In particular, HBBWP found that they needed to repeat each state in the PS scheme at least four times to get Heisenberg-limited scaling.

In the next section, we investigate the performance of our measurement scheme as discussed in Sec. II for different phase shifts and compare it with unentangled particles and HBBWP when  $\phi = 0$ .

#### IV. LOSSLESS RESULTS

The first stage of our scheme begins with the unentangled measurement; i.e.,  $N_u$  particles pass independently through a Mach-Zehnder interferometer with a phase,  $\phi$ , on path 1 and a (controllable) phase,  $\theta$ , on path 2. The probability of detecting particle  $i$  at output 1 is  $P_1 = \cos^2(\phi/2 - \theta_{i-1}/2)$  and at output 2 is  $P_2 = \sin^2(\phi/2 - \theta_{i-1}/2)$ , where  $\theta_{i-1}$  is the value  $\theta$  takes after the detection of the  $(i-1)$ th particle. After each detection event our phase distribution and hence phase estimate are modified. The process then continues by passing  $\gamma N_e$ -particle NOON states through the measurement scheme again using feedback to adjust  $\theta$  after each detection. From this  $\phi_{\text{est}}$  and  $\Delta\phi$  are determined.

By numerically optimizing  $N_u$ ,  $N_e$ , and  $\gamma$  (subject to the constraint  $N_T = N_u + \gamma N_e$ ) such that  $\Delta\phi$  is minimized we can determine the best precision afforded by this method for a given value of  $N_T$ . The exact form of the phase distribution, however, depends on the number of detections made at D1 and D2, meaning there will be variations between experiments. We take the phase distribution averaged over 200 runs in our simulations. The results are shown in Fig. 5(a) as a function of  $N_T$  for different values of  $\phi$ . We see that the precision is best for  $\phi = 0$  (as is also true for HBBWP). This is because in this case we have  $\theta = \phi$  for every measurement, whereas when  $\phi \neq 0$ , it takes a while for feedback to achieve this.

In Fig. 5(b), we have taken the case of  $\phi = 0$  and compared the results from our scheme [i.e., the solid line in Fig. 5(b)] with the case that all  $N_T$  particles are unentangled (dashed line) and the HBBWP scheme (crosses) where each state is repeated four times as discussed above. Only two points are displayed for HBBWP because they are the only values of  $N_T$  that correspond to this scheme on the range shown:  $N_T = 12$  corresponds to one- and two-particle states each repeated four times, and  $N_T = 28$  corresponds to one-, two-, and four-particle states each repeated four times. We see that, in the case of no loss, our measurement scheme outperforms the case of unentangled particles and gives a similar level of precision to the HBBWP scheme on the range shown. This is also true for phases other than  $\phi = 0$ , as we shall see in the next section.

However, so far everything has been treated by ignoring the effects of loss. One may also intuitively expect that our scheme will perform much better than PS or HBBWP in the presence of particle losses since these latter schemes use a large number of NOON states [22], which are known to be very fragile. By contrast, our scheme uses a large number of unentangled particles, which are more robust.

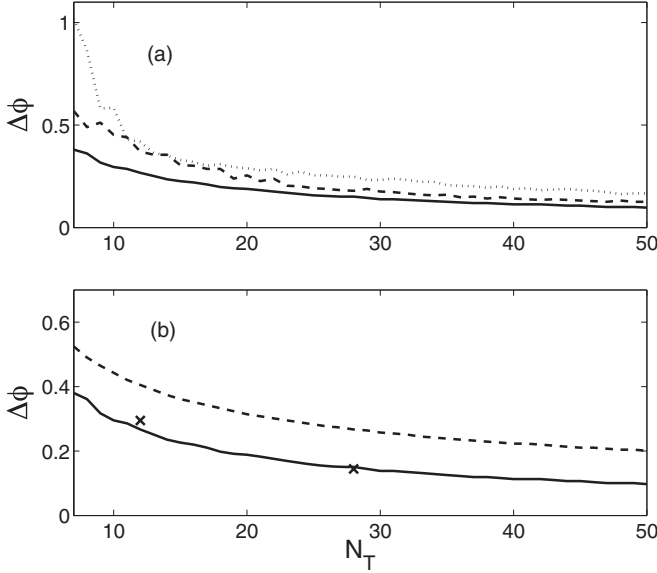


FIG. 5. (a) The measurement precision  $\Delta\phi$  as a function of  $N_T$  achieved using the optimum combination of  $N_u$ ,  $N_e$ , and  $v$  in our measurement scheme for  $\phi = 0$  (solid line),  $\phi = \pi/4$  (dotted line), and  $\phi = \pi/2$  (dashed line). The best precisions are achieved for  $\phi = 0$ ; however, the scheme holds its precision well over a range of phase values. (b) Comparison of the measurement precision  $\Delta\phi$  of our scheme (solid line), a scheme that uses only unentangled particles (dashed line), and the HBBWP scheme [11] (crosses), all for the case of  $\phi = 0$ .

## V. INCLUDING PARTICLE LOSSES

Particle losses are commonly modeled by placing “fictitious” beam splitters on each of the paths of the system, as shown in Fig. 6 [18,23–25]. If the beam splitter on path  $i$  has transmissivity  $\eta_i$ , it will skim off a fraction  $(1 - \eta_i)$  of the particles into environmental modes, which are then traced over.

A general two-mode NOON state with  $N_e$  particles (created by device 1) is transformed by the fictitious beam splitters and phase shifts  $\phi$  and  $\theta$  to

$$|\psi(\phi)\rangle = \frac{1}{\sqrt{2}} e^{iN_e(\phi-\theta)} \sum_{l_1=0}^{N_e} \binom{N_e}{l_1}^{1/2} \times \sqrt{\eta_1^{N_e-l_1} \sqrt{(1-\eta_1)^{l_1}}} e^{-il_1\phi} |N_e - l_1, 0\rangle_{1,2} |l_1, 0\rangle_{a,b}$$

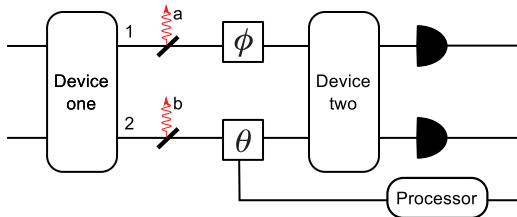


FIG. 6. (Color online) Schematic of the measurement scheme when particles on each path are lost to the environment. Losses are modeled by placing a fictitious beam splitter with transmissivity  $\eta_{1,2}$  on paths 1 and 2, respectively.

$$+ \frac{1}{\sqrt{2}} \sum_{l_2=0}^{N_e} \binom{N_e}{l_2}^{1/2} \sqrt{\eta_2^{N_e-l_2} \sqrt{(1-\eta_2)^{l_2}}} \times e^{-il_2\theta} |0, N_e - l_2\rangle_{1,2} |0, l_2\rangle_{a,b}, \quad (3)$$

where subscripts  $a$  and  $b$  refer to environmental modes, as shown in Fig. 6. For clarity, Eq. (3) represents the state just before device 2. Device 2 then acts to undo the unitary transformation of device 1. The state just after device 2 is then

$$|\psi(\phi)_{\text{out}}\rangle = \frac{1}{2} e^{iN_e(\phi-\theta)} \sum_{l_1=0}^{N_e} \binom{N_e}{l_1}^{1/2} \sqrt{\eta_1^{N_e-l_1} \sqrt{(1-\eta_1)^{l_1}}} \times e^{-il_1\phi} (|N_e - l_1, 0\rangle_{1,2} + |0, N_e - l_1\rangle_{1,2}) |l_1, 0\rangle_{a,b} + \frac{1}{2} \sum_{l_2=0}^{N_e} \binom{N_e}{l_2}^{1/2} \sqrt{\eta_2^{N_e-l_2} \sqrt{(1-\eta_2)^{l_2}}} \times e^{-il_2\theta} (|N_e - l_2, 0\rangle_{1,2} - |0, N_e - l_2\rangle_{1,2}) |0, l_2\rangle_{a,b}. \quad (4)$$

Once a particle is lost to the environment, we lose all information about that particle. Therefore we trace out environmental modes  $a$  and  $b$  to get

$$\rho(\phi)_{\text{out}} = \text{Tr}_{a,b} [|\psi(\phi)_{\text{out}}\rangle \langle \psi(\phi)_{\text{out}}|] = p_{\text{loss}} \rho_{\text{loss}} + p_{\text{no loss}} \rho_{\text{no loss}}, \quad (5)$$

where  $\rho_{\text{no loss}}$  is the density matrix of the system when no particles are lost,  $p_{\text{no loss}}$  is the probability of this occurring,  $\rho_{\text{loss}}$  is the density matrix of the system when one or more particles have been lost, and  $p_{\text{loss}} = 1 - p_{\text{no loss}}$ . Since we know that the loss of even a single particle completely destroys the NOON state superposition,  $\rho_{\text{loss}}$  cannot contain any phase information. Consequently, we need only consider  $\rho_{\text{no loss}}$  and  $p_{\text{no loss}}$  when determining the precision of NOON states. Experimentally, this is equivalent to ignoring all measurement results where we do not detect all  $N_e$  particles at the output. This is implicitly what happens in HBBWP, for example; however, here we fully account for all the resources used, including those that are not detected. Of course this means that we need to know if a particle is lost, which means that the detectors need to be sufficiently efficient. However, since our scheme uses small NOON states, this should not pose much of a problem. In HBBWP, for example, we just need to know whether a photon makes it to the detectors or not.

It is possible to show that  $\rho_{\text{no loss}} = |\psi_{nl}\rangle \langle \psi_{nl}|$ , where

$$|\psi_{nl}\rangle = \frac{1}{2\sqrt{p_{\text{no loss}}}} [(e^{iN_e(\phi-\theta)} \sqrt{\eta_1^{N_e}} + \sqrt{\eta_2^{N_e}}) |N_e, 0\rangle + (e^{iN_e(\phi-\theta)} \sqrt{\eta_1^{N_e}} - \sqrt{\eta_2^{N_e}}) |0, N_e\rangle] \quad (6)$$

and

$$p_{\text{no loss}} = (\eta_1^{N_e} + \eta_2^{N_e})/2. \quad (7)$$

It is reasonable to assume that the rate of loss is the same on both paths, and so we take  $\eta_1 = \eta_2 \equiv \eta$ . This simplifies  $|\psi_{nl}\rangle$  to

$$|\psi_{nl}\rangle = \frac{1}{2} [(e^{iN_e(\phi-\theta)} + 1) |N_e, 0\rangle + (e^{iN_e(\phi-\theta)} - 1) |0, N_e\rangle]. \quad (8)$$

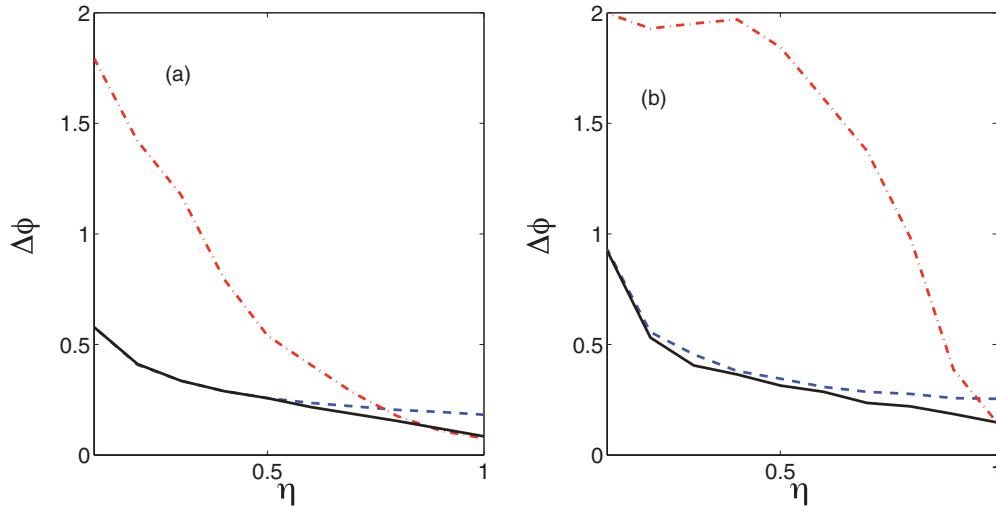


FIG. 7. (Color online) The precision achieved using our measurement scheme for different rates of loss (solid line) compared with the HBBWP scheme [11] (dash-dotted line) and a measurement scheme where all  $N_T = 60$  particles are unentangled (dashed line) when (a)  $\phi = 0$  and (b)  $\phi = \pi/3$ .

We can see from this (as we might expect since no particles are lost) that the probability of detecting all the particles at D1 is

$$P_{D1} = \cos^2 \left( \frac{N_e(\phi - \theta)}{2} \right) \quad (9)$$

and at D2 is

$$P_{D2} = \sin^2 \left( \frac{N_e(\phi - \theta)}{2} \right). \quad (10)$$

In our measurement system we have  $\gamma$  identical NOON states. However, not all  $\gamma$  runs will result in a successful measurement outcome, i.e., a detection of all  $N_e$  particles at the output. The probability of a particular run being successful is  $p_{\text{no loss}} = \eta^{N_e}$ . This means that our phase distribution is not updated on every run as in the idealized case. It is clear that larger NOON states are more rapidly affected by particle losses as the probability of a run being successful scales as  $\eta^{N_e}$ , meaning the larger the value of  $N_e$  is, the fewer successful runs there are.

Using this loss model, we have investigated the effects of particle loss on our measurement scheme and that of HBBWP. The precision capabilities of each scheme for different rates of loss are shown in Fig. 7 for  $N_T = 60$  and (a)  $\phi = 0$  and (b)  $\phi = \pi/3$ . In the HBBWP scheme, we use NOON states with particle numbers  $N_e = 1, 2, 4, \text{ and } 8$ , which are each repeated four times, as discussed above and noted in [11].

In the lossless case (i.e., when  $\eta = 1$ ) our scheme and HBBWP give almost identical results for both phases. This is consistent with the results presented in Fig. 5(b). However, the two schemes behave very differently when the rate of loss is increased. Our scheme retains its precision much better than HBBWP. Also shown in Fig. 7 is the precision obtained with unentangled particles (dashed line). This is a useful benchmark because it represents the shot-noise limit that we are aiming to beat. Our scheme is always at least as good as unentangled particles and is better over a wide range of loss rates. By contrast, the HBBWP scheme is

soon outperformed by unentangled particles as the loss rate is increased. The difference in performance is even more pronounced for  $\phi = \pi/3$  than  $\phi = 0$ .

One issue that we have skirted around thus far is whether the optimum strategy depends on the phase that we wish to measure. This would potentially be a problem because we do not know what this phase is to begin with and so would not know what strategy to employ. We have checked this over a range of parameters and found that the strategy does indeed vary with  $\phi$ . However, this is not as big a problem as it might appear. First, the variation is very slow. For example, using the values  $N_T = 60$  and  $\eta = 0.8$ , the optimum strategy always uses three-particle NOON states and between 21 and 30 single-particle states over the range  $\phi \in [0, \pi/2]$ . Second, we gain information about  $\phi$  as we implement our measurement and so can adapt the strategy as we go. Every scheme uses a significant number of single-particle states, and these can be used first to get an estimate of  $\phi$  and inform the later strategy of what size NOON states to use. For the example considered here with  $N_T = 60$  and  $\eta = 0.8$ , each strategy uses  $\sim 25$  single-particle states. These enable us to estimate  $\phi$  to within about  $\pi/\sqrt{25} = \pi/5$ , which is a better resolution than the range over which the strategy needs to be varied, i.e.,  $\sim \pi/2$ . In other words, by using the single-particle states first, we can determine  $\phi$  with sufficient precision that we can determine the optimum strategy as we go along without any loss of resources.

As a final comparison we relax the restriction that all the NOON states in our scheme must contain the same number of particles. This restriction was chosen to reduce the complexity of the scheme for possible experimental implementation. However, we should check that it does not significantly degrade the performance of the scheme. Instead we allow any combination of NOON states of different sizes subject to the restriction that the total number of particles is  $N_T$ . However, since NOON states are difficult to create experimentally for more than a few particles (and we want to ensure that we can determine when a particle is lost), we will restrict the NOON states to each contain no more than four particles. This makes

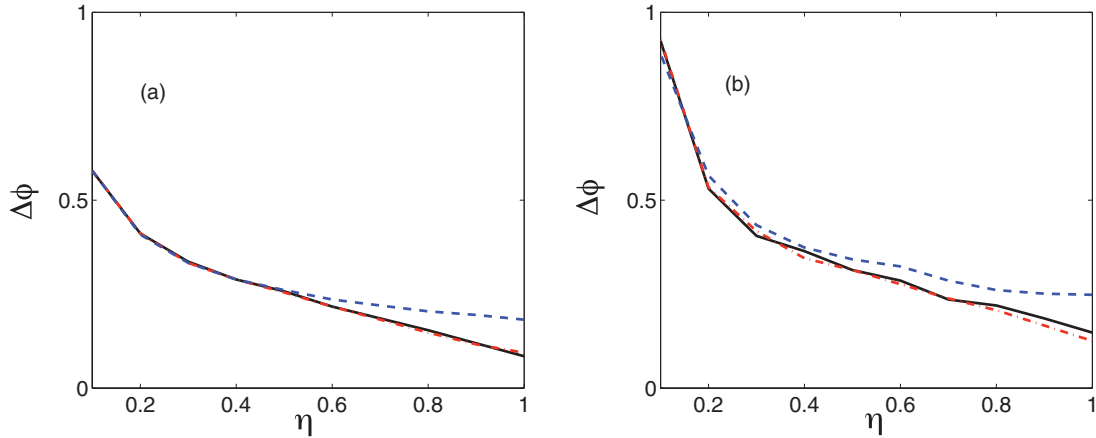


FIG. 8. (Color online) The precision achieved using our measurement scheme for different rates of loss (solid line) is compared with unentangled particles (dashed line) and the case of using any combination of NOON states where each contains a maximum of four particles (dash-dotted line) for (a)  $\phi = 0$  and (b)  $\phi = \pi/3$ . In both cases  $N_T = 60$ . In (a), the solid and dash-dotted lines are barely distinguishable.

the scheme experimentally plausible since four-photon NOON states have been realized in the laboratory [12].

The results are shown in Fig. 8. The scheme described here (dash-dotted line) is compared with our scheme described in the rest of the paper (solid line) where we restrict all NOON states to be the same size and the benchmark of unentangled particles (dashed line) for both  $\phi = 0$  [Fig. 8(a)] and  $\phi = \pi/3$  [Fig. 8(b)]. We see that the dash-dotted line gives only a marginal improvement over the solid line. This is particularly true for  $\phi = 0$ , where these two lines in Fig. 8(a) are barely distinguishable. This result justifies the scheme we have used throughout the paper that uses only unentangled states and NOON states of a fixed size. This scheme would be easier to implement than one that needs NOON states of different sizes, and yet it achieves almost the same measurement precision.

## VI. CONCLUSION

We have considered a practical scheme for measuring a completely unknown phase with sub-shot-noise precision in the presence of loss. We have used a bottom-up approach where we consider what states are experimentally accessible and see what we can achieve with them. This is in contrast to other approaches that calculate the theoretically optimal entangled states and then consider how these could be approximated in the laboratory.

We have focused, in particular, on unentangled particles and NOON states containing a small number of particles, and to simplify things further we have taken all our NOON states to be the same size. Our scheme is closely related to the work of PS [10] and HBBWP [11]; however, these latter schemes only consider the lossless case. In this paper, we have fully accounted for the resources required when there is loss and have shown that our scheme significantly outperforms the others when there is more than a modest rate of loss. This is important for all practical implementations of metrology where loss will inevitably be present. Finally, we have considered how our scheme compares to more general strategies that allow for NOON states with different sizes and found that our scheme compares very favorably with them. This justifies the use of our simpler approach.

All the schemes discussed in this paper make use of NOON states; however, it is known that different entangled states can combine Heisenberg-limited precision with enhanced robustness to particle loss. An interesting future direction will be to see how general entangled states can be incorporated into the measurement schemes discussed here and what advantages they provide in overall measurement precision [26].

## ACKNOWLEDGMENTS

This work was financially supported by DSTL. In addition, J.A.D. was supported by an RCUK fellowship, and J.J.C. was supported by a University of Leeds doctoral scholarship.

- 
- [1] V. Giovannetti, S. Lloyd, and L. Maccone, *Science* **306**, 1330 (2004).
  - [2] V. Giovannetti, S. Lloyd, and L. Maccone, *Nat. Photonics* **5**, 222 (2011).
  - [3] J. A. Dunningham, *Contemp. Phys.* **47**, 257 (2006).
  - [4] J. P. Dowling, *Contemp. Phys.* **49**, 125 (2008).
  - [5] S. Boixo, A. Datta, M. J. Davis, A. Shaji, A. B. Tacla, and C. M. Caves, *Phys. Rev. A* **80**, 032103 (2009).
  - [6] S. F. Huelga, C. Macchiavello, T. Pellizzari, A. K. Ekert, M. B. Plenio, and J. I. Cirac, *Phys. Rev. Lett.* **79**, 3865 (1997).
  - [7] J. Kolodyński and R. Demkowicz-Dobrzanski, *Phys. Rev. A* **82**, 053804 (2010).
  - [8] S. Knysh, V. N. Smelyanskiy, and G. A. Durkin, *Phys. Rev. A* **83**, 021804(R) (2011).
  - [9] B. M. Escher, R. L. de Matos Filho, and L. Davidovich, *Nat. Phys.* **7**, 406 (2011).

- [10] L. Pezzé and A. Smerzi, *Europhys. Lett.* **78**, 30004 (2007).
- [11] B. L. Higgins, D. W. Berry, S. D. Bartlett, H. M. Wiseman, and G. J. Pryde, *Nature (London)* **450**, 393 (2007).
- [12] T. Nagata, R. Okamoto, J. L. O'Brien, K. Sasaki, and S. Takeuchi, *Science* **316**, 726 (2007).
- [13] J. A. Dunningham and K. Burnett, *J. Mod. Opt.* **48**, 1837 (2001).
- [14] T. Kim, J. Dunningham, and K. Burnett, *Phys. Rev. A* **72**, 055801 (2005).
- [15] We see from this that as the total number of particles gets large, the number of unentangled particles  $N_u$  will dominate, and so we will approach the shot-noise limit. This scheme therefore works when the number of particles is not too large.
- [16] The optimal states for phase sensing with loss (where the phase is initially well known) have been calculated in [24,25] and also have the form of a series of small NOON states.
- [17] S. L. Braunstein, C. M. Caves, and G. J. Milburn, *Ann. Phys. (N.Y.)* **247**, 135 (1996).
- [18] R. Demkowicz-Dobrzanski, U. Dorner, B. J. Smith, J. S. Lundeen, W. Wasilewski, K. Banaszek, and I. A. Walmsley, *Phys. Rev. A* **80**, 013825 (2009).
- [19] C. R. Rao, *Bull. Calcutta Math. Soc.* **37**, 81 (1945).
- [20] H. Cramér, *Mathematical Methods of Statistics* (Princeton University Press, Princeton, NJ, 1946).
- [21] C. W. Helstrom, *Quantum Detection and Estimation Theory* (Academic, New York, 1976).
- [22] Strictly, the HBBWP does not use a NOON state but a single-particle state that makes multiple passes through the phase. However, the same argument holds. The multipass state is more susceptible to losses since, if the particle is lost on any one of the multiple passes, the entire state is destroyed. This is much like a NOON state, where the loss of a single particle destroys the whole state.
- [23] S. D. Huver, C. F. Wildfeuer, and J. P. Dowling, *Phys. Rev. A* **78**, 063828 (2008).
- [24] U. Dorner, R. Demkowicz-Dobrzanski, B. J. Smith, J. S. Lundeen, W. Wasilewski, K. Banaszek, and I. A. Walmsley, *Phys. Rev. Lett.* **102**, 040403 (2009).
- [25] T. W. Lee, S. D. Huver, H. Lee, L. Kaplan, S. B. McCracken, C. Min, D. B. Uskov, C. F. Wildfeuer, G. Veronis, and J. P. Dowling, *Phys. Rev. A* **80**, 063803 (2009).
- [26] G. Y. Xiang, B. L. Higgins, D. W. Berry, H. M. Wiseman, and G. J. Pryde, *Nat. Photonics* **5**, 43 (2011).